AIP Journal of Applied Physics

Investigation of polarization switching in (001) c , (110) c , and (111) c oriented Pb(Zn 1/3 Nb 2/3) O 3 –4.5% PbTiO 3 crystals

Christelle Jullian, J. F. Li, and D. Viehland

Citation: Journal of Applied Physics **95**, 5671 (2004); doi: 10.1063/1.1699500
View online: http://dx.doi.org/10.1063/1.1699500
View Table of Contents: http://scitation.aip.org/content/aip/journal/jap/95/10?ver=pdfcov
Published by the AIP Publishing

Investigation of polarization switching in $(001)_c$, $(110)_c$, and $(111)_c$ oriented $Pb(Zn_{1/3}Nb_{2/3})O_3-4.5\%PbTiO_3$ crystals

Christelle Jullian, J. F. Li, and D. Viehland[a)]
Department of Materials Science and Engineering, Virginia Tech, Blacksburg, Virginia 24061

(Received 7 November 2003; accepted 15 February 2004)

The dynamics of polarization switching have been investigated over extremely broad time ($10^{-8}<t<10^2$ s) and field ranges for $(001)_c$, $(110)_c$, and $(111)_c$-oriented $Pb(Zn_{1/3}Nb_{2/3})O_3-4.5\%PbTiO_3$ crystals. The results demonstrate the presence of broad relaxation time distributions that can extend over a decade(s) in orders of magnitude in time, and which sharpen significantly with increasing field. The polarization transients have been fit to stretched exponential functions, which are typical of disordered systems. © *2004 American Institute of Physics.* [DOI: 10.1063/1.1699500]

I. INTRODUCTION

Oriented poled single crystals of $(1-x)Pb(Zn_{1/3}Nb_{2/3})O_3-xPbTiO_3$ (PZN–x%PT) and $(1-x)Pb(Mg_{1/3}Nb_{2/3})O_3-xPbTiO_3$ (PMN–x%PT) have attracted attention because of enormous piezoelectric ($d_{33}\sim1800$ pC/N) and electromechanical coupling ($k_{33}\sim0.94$) coefficients.[1,2] Maximum property coefficients are found in the vicinity of a morphotropic phase boundary between rhombohedral and tetragonal ferroelectric phases. The enormous responses have been attributed to the presence of intermediate monoclinic (FE_M) ferroelectric phases.[3–7] Several monoclinic phases have been found, including: (i) a FE_{Mc} with the polarization constrained to the $(110)_c$ plane, (ii) a FE_{Ma} with the polarization constrained to $(010)_c$, and (iii) a FE_{Mb} with the polarization constrained to $(100)_c$, which has been found only for $(110)_c$-oriented crystals under field.

Polarization rotation instabilities under field within FE_M phases[8,9] are known, where rotation occurs against a very small anisotropy, and thus the hysteresis is negligible. For a field applied along $(001)_c$, the rotational pathway has been predicted to be $FE_{Ma}\rightarrow FE_{Mc}\rightarrow FE_t$. Investigations of the induced polarization (P) have shown significant differences depending upon whether the crystals are driven under a unipolar or bipolar electric field (E).[10–12] For both $(001)_c$- and $(110)_c$-oriented crystals, unipolar drive results in anhysteretic $P-E$ responses, whereas bipolar drive results in significant hysteresis. Clearly, domains are important in polarization switching under bipolar drive, however most investigations have focused on unipolar operation.

A. Prior studies of polarization dynamics in normal ferroelectrics

Polarization switching has been extensively investigated in normal ferroelectric materials by measuring current transients in response to square wave electrical pulses of a reverse electric field.[13–20] The kinetics have been modeled using a modified Avrami equation, given as

$$J(t)=(2P_0n/\tau)(t/\tau)^{n-1}\exp[-(t/\tau)^n], \tag{1a}$$

or

$$P(t)=P_0\exp[-(t/t)^n], \tag{1b}$$

where $J(t)$ is the current density as a function of time, $P(t)$ is the polarization as a function of time, P_0 is the induced polarization, n is the dimensionality of the switching process, τ is the characteristic relaxation time, and t is the elapsed time since the application of the electric field.

However, limiting the study of domain dynamics and polarization switching has been that current transient investigations have been performed over relatively narrow time (t) and electric field (E) ranges[13–20]—even though the current response is known to be logarithmic in time.[18,21–24] An analysis of the dynamics in the time domain of $10^{-8}<t<10^{-6}$ s has provided incomplete information, upon which to develop a mechanistic understanding. Various investigations have used Eqs. 1(a) and 1(b). Early investigations by Mertz[13] revealed a model for polarization reversal where two-dimensional (2D) nucleation of reversed clusters occurs on existing 180° domain walls and where one-dimensional growth of reversed steplike domains occurs perpendicular to the direction of E. In this model, nucleation is confined to the domain wall and, during domain growth, the twin wall is restricted to be coherent, as illustrated in Fig. 1. It is known that in finite-size systems that the Mertz model is inapplicable,[25] and has been extended by Scott *et al.*[26] to account for spatially limited conditions.

An analysis of data has resulted in important differences about what should be expected using Eqs. 1(a) and 1(b). First, an analysis has shown fractal exponents, whereas strict use of Eqs. 1(a) and 1(b) requires integer values. A recent analysis by Shur *et al.*[16] attempted to resolve this difference by allowing n to change between integer values. This change was attributed to a geometric catastrophe, conjectured to result from domain impingement. Second, an analysis revealed that nucleation and growth is at most a 2D process, generally with an average dimensionality constant of ~1.5. However, both homogeneous and heterogeneous nucleation and growth are volume [i.e., three-dimensional (3D)] processes. Finally,

a)Electronic mail: dviehlan@vt.edu

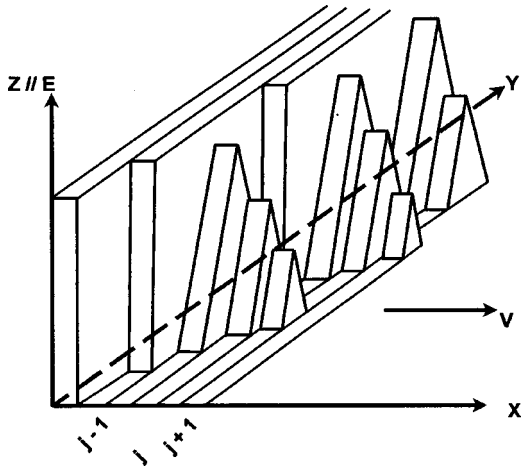

FIG. 1. Mertz model of domain nucleation and growth (see Ref. 13). An electric field is applied parallel to the *z* axis; the symbols j−1, j, and j+1 represent domain wall steps; the domain-wall motion occurs in a sidewise manner along the *x* and *y* axes; and the domain-wall velocity along the *x* direction is represented by the symbol *v*.

an analysis of ferroelectric switching currents with Eqs. 1(a) and 1(b) tended to underpredict the current at longer times of $t>4t_{\max}$, where $t_{\max}$ is the time of the current maximum. This results in a skewing of the current transient peaks to longer times in the time domain of $10^{-8}<t<10^{-6}$ s.[16,18–20]

B. Prior studies of polarization dynamics in PMN–*x*%PT

In the ferroelectric domain theory, the importance of defects has been considered[27] as preferred nucleation sites. Prior investigations[24] have shown a stage in polarization switching that depends logarithmically on time. But, not until recent studies by Scott *et al.*[26] and by Viehland *et al.*[22,23] have defects been considered to play a vital role in polarization dynamics.

Recently, in PMN–*x*%PT, skewing has been understood by stretched exponential functions that include the effect of random fields which broaden nucleation and growth events in the time domain.[22] Also, recent *P*–*E* studies have revealed pronounced dispersion in the frequency domain of $10^{-2}<f<10^{2}$ Hz.[23] The polarization dynamics and frequency relaxation of PMN–*x*%PT have been analyzed using stretched exponential functions[28–30] which have terms in $[\ln(t/\tau)]^n$, given as

$$P(t)=P_0\exp\{-a[\ln(t/\tau)]^n\}, \tag{2}$$

where $P(t)$ is the time dependence of the polarization, P_0 is the total nucleated polarization, and *a* is an exponential factor. This equation has similarities to the Avrami relationship given in Eq. 1(b), where terms in $(t/\tau)^n$ have been replaced by ones in $[\ln(t/\tau)]^n$. Substitution with $\ln(t/\tau)$ will result in a significant extension to longer times of the long-time tail of the nucleation curve, relative to a similar relationship in terms of (t/τ). Equation (2) also predicts that $\ln(P)$ depends on $[\ln(t)]^n$, which will result in significantly stronger broadening in the time domain than a simple dependence of *P* on $n\ln(t)$.

Stretched exponential behavior is well known in disordered systems.[31–33] It is a form of hierarchial relaxation. In the random-field theory, the nucleation of domain boundaries under field occurs in the vicinity of quenched defects that are conjugate to the applied ordering field. Consequently, domain walls become diffuse and polar nanoregions (PNRs) can be created. Many modified perovskite ferroelectrics are known to contain significant quenched disorder, such as PMN–*x*%PT and PZN–*x*%PT.[34–37] Interestingly, electron microscopy studies of poled soft ferroelectrics ceramics by Tan *et al.*[38] have previously shown domain breakdown with increasing ac electric field, which is consistent with polarization switching through a relaxor state. After a weak field drive, normal micron-sized domains were found. However, after a modest ac drive (1–3 kV/cm), specimens of the same composition were found to consist of PNRs. Correspondingly, dielectric constant measurements under a weak field drive exhibited normal ferroelectric behavior, where as that under 1–3 kV/cm exhibited relaxor behavior.

C. Purpose of investigation

Investigations of polarization dynamics of PMN–*x*%PT or PZN–*x*%PT for variously oriented crystals have not yet been performed. Such studies could provide important information concerning the mechanism of switching. In this investigation, we report the polarization dynamics over a broad time domain extending from $10^{-8}<t<10^{2}$ s for $(001)_c$-, $(110)_c$-, and $(111)_c$-oriented PZN–4.5%PT crystals. Studies were performed from $E\ll E_c$ to $E\gg E_c$, where E_c is the coercive field. The results demonstrate the presence of extremely broad relaxation time distributions for the switching process, extending over a decade(s) in orders of magnitude in time, where the distribution is strongly dependent on *E*.

II. EXPERIMENTAL PROCEDURE

Single crystals of $Pb(Zn_{1/3}Nb_{2/3})O_3$–4.5%$PbTiO_3$ (PZN–4.5%PT) grown by a Bridgeman method were obtained from TRS Ceramics (State College, PA). The crystals were of various orientations, including $(001)_c$, $(110)_c$, and $(111)_c$. The specimens were cut into typical dimensions of 0.3 mm in thickness and 4 mm^2 in area, and were electroded with gold. *P*–*E* measurements were made using a modified Sawyer–Tower bridge. This system was computer controlled and capable of automatic determination of standard *P*–*E* measurement compensation parameters. The system was capable of the precise measurement of the *P*–*E* response over the frequency range from 10^{-3} to 10^{2} Hz, the charge range from ~10 pC to 100 μC, and the current range from ~1 nA to 10 mA. A sinusoidal driving field was used.

The specimens were also studied using a current transient method. Investigations were performed for various fields of $0<E<3E_c$. In order to measure the response of the specimens over a broad time domain from $10^{-8}<t<10^{2}$ s, three different measurements circuits were developed and built.[39] Figure 2(a) shows the measurement circuit for the short-time domain between 10^{-8} to 10^{-6} s. Figure 2(b) shows the circuit for the middle-time domain between 10^{-6} and 10^{-3} s. And, Fig. 2(c) shows the circuit for the long-time

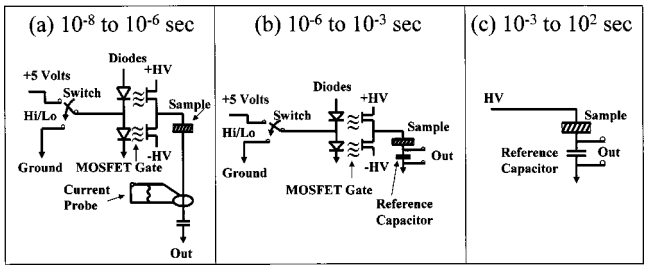

FIG. 2. Measurement circuit of switching current responses for the various time domains: (a) Short-time domain between $10^{-8}<t<10^{-6}$ s, (b) middle-time domain between $10^{-6}<t<10^{-3}$ s, and (c) long-time domain between $10^{-3}<t<10^{2}$ s. The circuits behind the specimen are equivalent for the short- and middle-time domains. This circuit consists of a switch, rapid response diodes, and metal–oxide–semiconductor field-effect transistor (MOSFET) gates. In the fast time domain, a current probe is used to lower the input voltage into an oscilloscope. For the middle- and long-time domains, the circuits in front of the specimen are equivalent. The voltage is measured across a reference capacitor, using an oscilloscope operated in a time capture mode.

domain between 10^{-3} and 10^{2} s. For the short- and middle-time domains, the same procedure was used prior to switching. Initially, the specimen was unpoled, and then an electric field of $-3E_c$ was applied to repole the specimen. To prepare for switching, both sides of the specimen were raise to the desired switching field. Then, at time $t=0$, one side of the specimen was taken to ground: This is an important step that allowed for the very highest current wall between the power amplifier and the specimen. By using these steps, we can certify that the high voltage reaches its full maximum, before the polarization starts to rise. It was found that switching times of $\ll 10^{-8}$ s could be achieved. For the long-time domain, this method could also be used, but is not necessary as the rise time of the amplifier is significantly shorter than the measurement time. An Agilent oscilloscope operated in a time capture mode was used to measure the output voltage from each circuit.

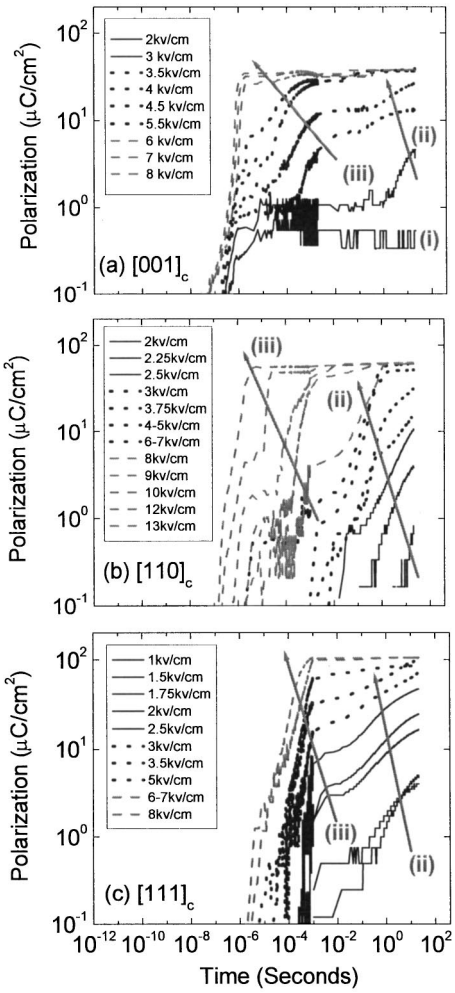

FIG. 3. Logarithm of polarization as a function of logarithm of time for various oriented PZN–4.5%PT crystals over broad time and field ranges: (a) Along $(001)_c$, (b) along $(110)_c$, and (c) along $(111)_c$. Data are shown for three different field regimes of $E<E_c$, $E\approx E_c$, and $E>E_c$ regimes in each figure.

III. RESULTS

A. Time domain

Figures 3(a)–3(c) respectively show the logarithm of the polarization as a function of the logarithm of time for PZN–4.5%PT crystals oriented along the $(001)_c$, $(110)_c$, and $(111)_c$. Data are shown for over ten decades in time, taken at various applied electric fields. The polarization curves can clearly be seen to be extremely broad in the time domain, extending over a decade(s) of orders in magnitude. The curves sharpened at higher fields of $E\gg E_c$. Unambiguously, polarization switching for PZN–4.5%PT crystals has a very broad distribution of relaxation times τ. The breadth of this distribution is nearly equal to that found in the weak-field susceptibility (dielectric constant) of relaxor ferroelectrics near their freezing temperature.[40–42] However, there were important differences between the polarization curves for the variously oriented crystals.

1. Small fields applied along various orientations

At lower fields of $E\approx 2$ kV/cm applied along the $(001)_c$, the transient had a fast change at $t\approx 10^{-6}$ s and was independent of time for $t>10^{-5}$ s. This transient is indicated by (i) in Fig. 3(a). Whereas, along the $(110)_c$ and $(111)_c$, the time constant of the transient was dramatically longer near this field level—on the order of 1 to 10^{2} s. These transients are indicated by (ii) in Figs. 3(b) and 3(c), respectively. The results clearly indicate an important difference between the variously oriented crystals. *Along* $(001)_c$, *a rapid change in polarization occurs under a modest electric field pulse, whereas such changes along* $(110)_c$ *and* $(111)_c$ *are dramatically slower*.

2. Increasing E applied along (001)c

For a field of $E=3$ kV/cm applied along $(001)_c$, a long-time polarization transient can be seen in the time domain of $1<t<10^{2}$ s, as indicated in Fig. 3(a) by the symbol (ii). With increasing field for $3<E<5$ kV/cm, this long-time polarization transient was found to shift to shorter times. In addition, for $3<E<5$ kV/cm, a third transient was observed in the intermediate time domain of $10^{-5}<t<10^{-3}$ s, as indicated in Fig. 3(a) by the symbol (iii). This intermediate-time transient also shifted to shorter times with increasing E.

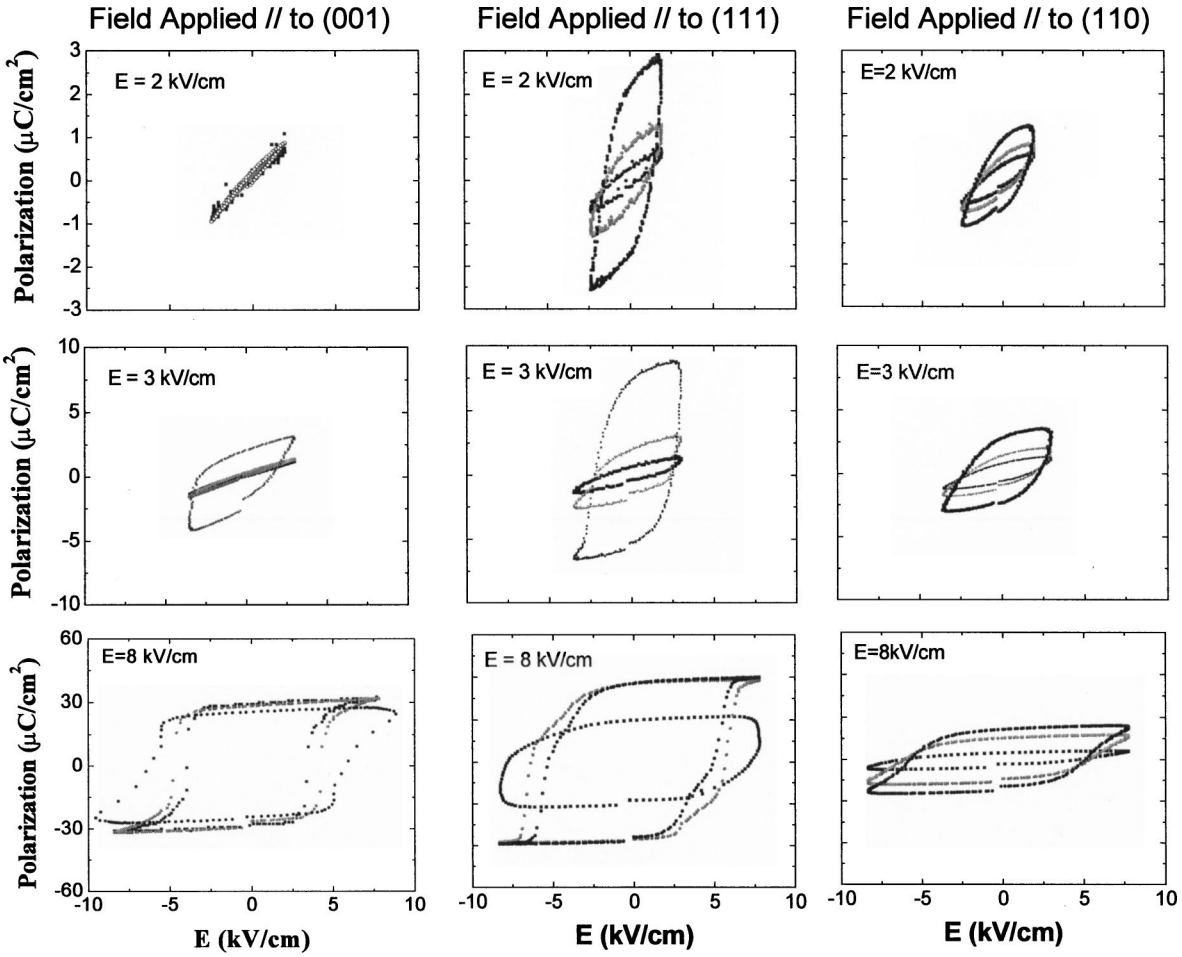

FIG. 4. Panel of $P-E$ curves for various oriented PZN–4.5%PT crystals. The left-hand side column is for a $(001)_c$ oriented crystal, the middle for a $(111)_c$, and the right for a $(110)_c$. Data are shown at various maximum drive levels, where each row on the panel was taken under a constant maximum E. The top row was for 2 kV/cm, the middle for 3 kV/cm, and the bottom for 8 kV/cm. In each figure, data are shown for various measurement frequencies of 10^{-2}, 1, and 10^2 Hz.

For $3<E<5$ kV/cm, *the results show that a very rapid polarization response occurred at short times, followed by a delay, an intermediate-time transient, another delay and, finally, a long-time transient*. With increasing E in this range, the three polarization process can be seen to gradually merge at shorter times. For $E>6$ kV/cm, a single rapid ballistic polarization response was observed, whose time constant was $\sim 10^{-6}$ s.

3. Increasing E applied along $(110)_c$ and $(111)_c$

Only two evolutionary stages in the time domain were found during polarization switching with increasing E applied along $(110)_c$ and $(111)_c$. At low fields, a long-time transient was found which shifted to shorter times with increasing E, as discussed in a preceding subsection, and indicated by the symbol (ii) in Figs. 3(b) and 3(c). For higher E, a second transient developed in the time domain of 10^{-4} s, as indicated by the symbol (iii) in Figs. 3(b) and 3(c). *The results demonstrate a broad polarization transient in the intermediate time domain, followed by a delay, and a subsequent second broad polarization transient in the long-time domain.*

It is important to note that long-time polarization transients were present in much lower fields along $(111)_c$, than along $(110)_c$. *Clearly, there is an ease of the polarization response in the long-time domain along* $(111)_c$ *for fields of* $E \ll E_c$. In fact, over the entire time-domain investigated, under the same applied field, the polarization response along $(111)_c$ was noticeably more rapid than that along $(110)_c$. At high fields, the two broad polarization transients can be seen to gradually merge, and a single more rapid polarization response becomes evident.

In addition, along both $(111)_c$ and $(110)_c$, the leading edge of the polarization response at short times was noticeably field dependent, decreasing from $\sim 10^{-3}$ to $\sim 10^{-6}$ s with increasing field between ~3 to ~12 kV/cm. Such a pronounced shift in the leading edge of the polarization response was not found along $(001)_c$, as its edge was always in the range of 10^{-6} s.

B. Frequency domain

Figure 4 shows a panel of $P-E$ curves. The left-hand side column shows those along $(001)_c$, the middle column; $(110)_c$, and the right-hand side one; $(111)_c$. There are also three rows shown in the panel which represent different maximum ac electric fields. The first row was for 2 kV/cm,

the second; 3 kV/cm, and the third; 8 kV/cm. Each figure in the panel contains data taken at frequencies of 10^{-2}, 1, and 10^2 Hz.

1. Increasing E applied along $(001)_c$

For $E \approx 2$ kV/cm applied along $(001)_c$, a linear $P-E$ response was found that was frequency independent. Also, the $P-E$ response was anhysteretic. The induced polarization was ~ 0.01 C/m^2. The large amplitude dielectric constant can be calculated as

$$K = \frac{P}{\epsilon_0 E} = \frac{10^{-2}\ \text{C/m}^2}{8.85\times 10^{-12}\ \text{F/m}\ \ 10^5\ \ \text{V/m}} \approx 5000,$$

where ϵ_0 is the permittivity of free space. This large signal value of K was found to be equivalent to the weak-field one measured using an Agilent 4284 LCR meter. This demonstrates that the $P-E$ response along $(001)_c$ is a near ideal linear dielectric for $E<2$ kV/cm. Also, these results measured in the frequency domain are consistent with corresponding ones in the time domain, shown in Fig. 3(a). The lack of time dependence for $t>10^{-5}$ s is in agreement with the frequency independent response in the range of $10^{-2} < f < 10^2$ Hz. The anhysteretic nature of the $P-E$ response along $(001)_c$ demonstrates that the polarization mechanism is essentially nondissipative for $E<2$ kV/cm.

Near ideal linear $P-E$ behavior was observed along $(001)_c$ with increasing E to 3 kV/cm. However, nonlinearity and hysteresis became apparent at a low frequency. The onset of hysteresis corresponded to the appearance of a long-time polarization transient in the time domain data near $1 < t < 10^2$ s, as illustrated in Fig. 3(a) by the symbol (ii). As E was increased, significant hysteresis became apparent at increasingly lower frequencies. At higher fields, complete switching was observed in the $P-E$ response. But, E_c was notably frequency dependent, shifting to higher values with increasing frequency, as previously reported for PMN–x%PT.[23] The results in the left-hand side panel of Fig. 4 clearly show a transition with increasing field from a dynamical polarization process which is nondissipative and linear, to one which is dissipative and nonlinear.

2. Increasing E applied along $(110)_c$ and $(111)_c$

However, for $E \leqslant 2$ kV/cm applied along either $(110)_c$ or $(111)_c$, a nonlinear $P-E$ response was found which was strongly frequency dependent and hysteretic. Consider, for example, a field of $E=1$ kV/cm applied along $(111)_c$, the induced polarization was ~ 0.03 C/m^2 at 10^{-2} Hz, which decreased to ~ 0.005 C/m^2 at 10^2 Hz. Correspondingly, the hysteretic losses decreased with increasing frequency. It is important to note that these frequency domain results are consistent with the corresponding time domain ones, which revealed long-time polarization transients in the time range of $10^{-2} < t < 10^2$ s for $E=2$ kV/cm. The pronounced hysteresis in the $P-E$ response along $(111)_c$ and $(110)_c$ demonstrates that the long-time polarization transients are strongly dissipative. With increasing E to 3 kV/cm, the degree of polarization relaxation in the $P-E$ response was found to increase. This increase corresponds to a shift to shorter times of the long-time polarization transient.

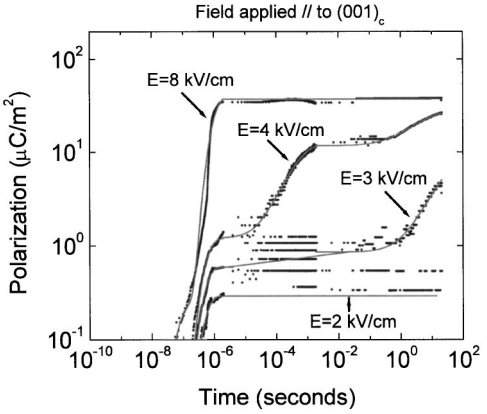

FIG. 5. Fitting of the logarithm of polarization as a function of logarithm of time to Eq. (2) for a PZN–4.5%PT crystal in response to a square wave pulse applied along $(001)_c$. Data are shown for various maximum fields of 2 kV/cm, 3 kV/cm, 4 kV/cm, and 8 kV/cm.

IV. FITTING OF CURRENT TRANSIENTS TO STRETCHED EXPONENTIAL FUNCTIONS

The time domain polarization data of Fig. 3 were fit to Eq. (2), using a Levenberg–Marquadt nonlinear analysis. Multiple stretched exponential contributions were allowed for each data set. Two were sufficient to obtain good fitting to Eq. (2) along $(111)_c$ and $(110)_c$, whereas three were required along $(001)_c$. As discussed in Sec. III, all three orientations had broad intermediate ($10^{-4} < t < 10^{-2}$ s) and long-time polarization transients ($t>1$ s). In addition, along $(001)_c$, a third transient was found at short times of $t \approx 10^{-6}$ s.

The fitting of Eq. (2) to the data are shown in Figs. 5–7 for fields applied along $(001)_c$, $(111)_c$, and $(110)_c$, respectively. Four data sets are shown in Figs. 5–7 to illustrate the changes in the time-domain polarization response with increasing E. The fitting to Eq. (2) is shown as a solid line in

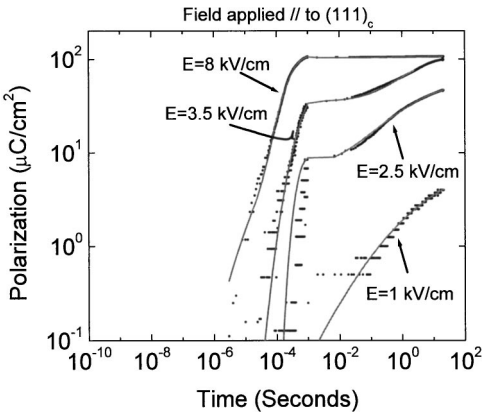

FIG. 6. Fitting of the logarithm of polarization as a function of logarithm of time to Eq. (2) for a PZN–4.5%PT crystal in response to a square wave pulse applied along $(111)_c$. Data are shown for various maximum fields of 1 kV/cm, 2.5 kV/cm, 3.5 kV/cm, and 8 kV/cm.

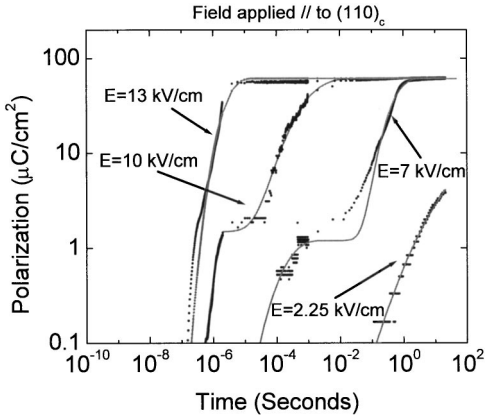

FIG. 7. Fitting of the logarithm of polarization as a function of logarithm of time to Eq. (2) for a PZN–4.5%PT crystal in response to a square wave pulse applied along $(110)_c$. Data are shown for various maximum fields of 2.25 kV/cm, 7 kV/cm, 10 kV/cm, and 12 kV/cm.

the plots, and the experimental data as small points. Inspections of Figs. 5–7 will reveal a very good fitting of the data to Eq. (2). This demonstrates that polarization switching in PZN–x%PT occurs by an extremely broad relaxation time distribution, typical of a stretched exponential function (2); rather than by a simple relaxation process with a well-defined singular relaxation time, typical of the Avrami Eq. (1). High confidence levels were found in the fittings to Eq. (2) ($R^2 \approx 0.99$).

A. Average relaxation time

The average relaxation time, τ, obtained from the fitting to Eq. (2) is shown in Figs. 8(a)–8(c) as a function of E^{-1} along $(001)_c$, $(110)_c$, and $(111)_c$, respectively. Along each direction, there was more than one average relaxation time. This is because each data set required more than one stretched exponential contribution. The value of τ is shown in Figs. 8(a)–8(c) for every polarization transient in the respectively oriented specimens. The field dependent relaxation time τ was analyzed with a modified Arrhenius equation, given as

$$\tau = \tau_0 \exp[-E_0/E], \tag{3}$$

where τ_0 is the nucleation attempt frequency, and E_0 is the activation field barrier.

Along $(001)_c$, the rapid polarization response was found to have a value of $\tau \approx 10^{-6}$ s, which was nearly unchanged with increasing E. This reflects the fact that the leading edge of the polarization response in the time domain was nearly independent of E over the range of fields investigated. An analysis with Eq. (3) yielded a value of $\tau_0 \approx 10^{-6}$ s and an activation field of $E_0 \approx 0$ kV/cm. The magnitude of the polarization switched by this rapid process varied significantly with E, however the kinetics of the response were essentially unaltered by E. These results demonstrate that this polarization mechanism, which was observed only along $(001)_c$ under low fields, has an extremely low, or possibly no, nucleation barrier.

An analysis with Eq. (3) was also performed on the long- and intermediate-time polarization transients along all three orientations. The intermediate-time transients yielded close to the same value of $\tau_0 \approx 10^{-4}$ s along all three directions. There were differences in the value of E_0. Along $(001)_c$ and $(110)_c$, the values of the activation field were $E_0 \sim 10$ kV/cm, whereas along $(111)_c$ it was notably lower with $E_0 \approx 6.5$ kV/cm. The long-time transients gave close to the same value of $\tau_0 \approx 10^{-2}$ s along all three directions. Again, there was differences in the value of E_0, which was $\sim$10 kV/cm along both $(001)_c$ and $(110)_c$, but was notably lower with $E_0 \approx 2$ kV/cm along $(111)_c$. The significantly lower value of E_0 along $(111)_c$ explains why there is an ease of the polarization response in the long-time domain for $E \ll E_c$—the nucleation barrier, under modest to high fields, is lower along $(111)_c$ than the other orientations.

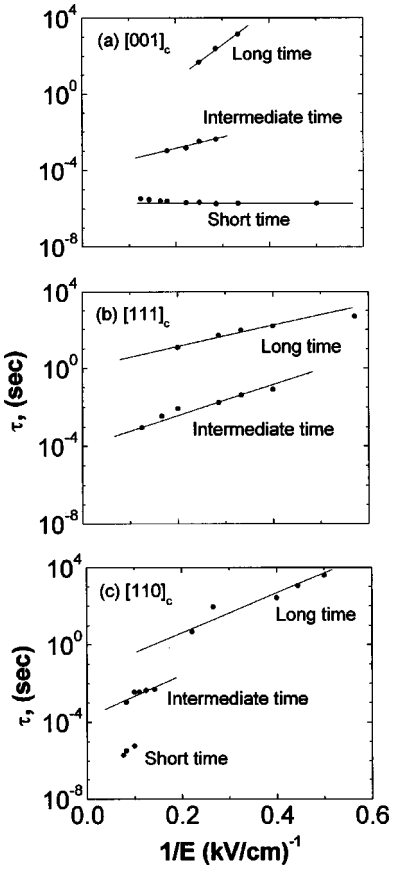

FIG. 8. Dimensionality constant, n, as a function of applied field for PZN–4.5%PT taken along (a) $(001)_c$, (b) $(111)_c$, and (c) $(110)_c$.

B. Dimensionality

The dimensionality factor, n, obtained from the fitting to Eq. (2) is shown in Figs. 9(a)–9(c) as a function of E along $(001)_c$, $(110)_c$, and $(111)_c$, respectively. It is important to note that n was consistently found to be very close to an integer value.

Along $(001)_c$, the rapid polarization response ($t < 10^{-6}$ s) at low E was found to have a dimensionality constant of $n \approx 3$. This demonstrates that the nonactivated polarization response along this direction at low E is a volume process. At modest E, applied along all three orientations studied, the long-time polarization transients ($t \sim 10^{-2}$ s)

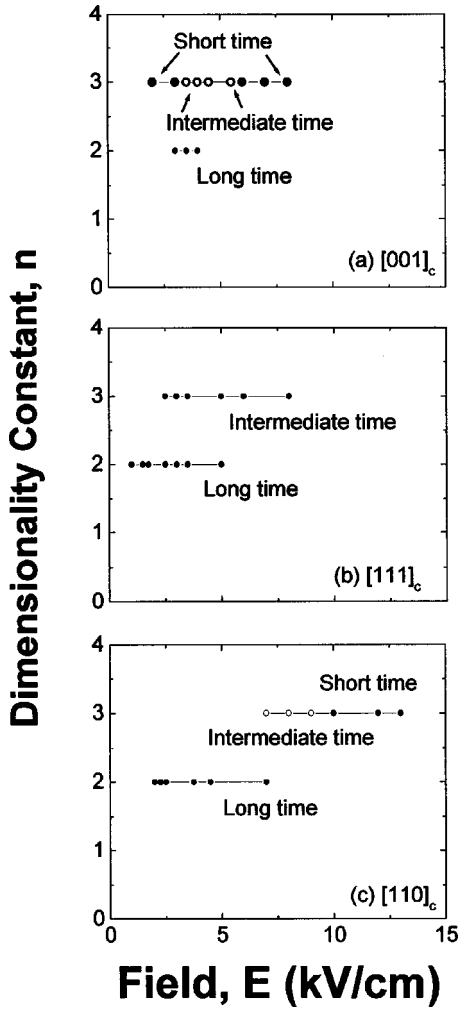

FIG. 9. Logarithm of the relaxation time, τ, as a function of applied field for PZN–4.5%PT taken along (a) $(001)_c$, (b) $(111)_c$, and (c) $(110)_c$.

were found to have a dimensionality constant of $n \approx 2$. However, at higher E applied along all three orientations, the intermediate-time polarization transients ($t \sim 10^{-4}$ s) were found to have a dimensionality of $n \approx 3$.

V. DISCUSSION AND SUMMARY

Our results support a model of polarization switching in PZN–4.5%PT crystals by continuous renucleation, or a nucleation limited model, rather than a domain growth process. The polarization transient data presented are indicative of one reversible polarization event at low E along $(001)_c$, and two types of nucleation events with increasing E along all orientations investigated. Our data indicate that all polarization events are broad in the time domain, following stretched exponential behavior.

A. Polarization rotation under small fields along $(001)_c$, $FE_{Ma} \rightarrow FE_R$ transition

Along $(001)_c$, under a small reverse field, a rapid polarization response ($t < 10^{-6}$ s) occurs heterogeneously throughout the volume of the crystal ($n = 3$). However, it is unlike nucleation, in that it has no activation barrier—it is reversible and nondissipative.

We can try to understand this by considering polarization rotation in the FE_{Ma} phase of PZN–4.5%PT. The polarization lies close to the $(111)_c$, but is slightly rotated toward $(001)_c$. Under a small applied reverse E, polarization rotation can occur in the $(010)_c$ plane. It can rotate toward $(111)_c$ under reverse field, or toward $(001)_c$ under a forward field. The nucleation barrier for polarization rotation is low, as the anisotropy in the $(100)_c$ plane is small.[8,9] Nuclei with a reversed polarization are not created under small reverse E; rather the polarization vector of pre-existing domains rotates.

B. Creation of nuclei with reversed polarization with increasing *E* along various orientations

Under moderate pulse heights applied along $(001)_c$, a boundary nucleation process ($n = 2$) became evident on long time scales of $t > 10^{-2}$ s. A similar polarization transient in this time-domain region was also found along $(110)_c$ and $(111)_c$. This process appears to be the creation of domain nuclei with a reversed polarization. It is dissipative, as evidenced by hysteresis in the $P-E$ curves. Under moderate E, the creation of nuclei with a reversed polarization seemingly occurs. This nucleation is geometrically confined to preexisting domain boundaries ($n = 2$). The nucleation events have a broad relaxation time distribution. The events may be confined to domain walls, but nucleation results in a long-time (creeplike) response to E. Thus, domain walls should become spatially nonuniform or diffuse with time.

With a further increase in pulse height applied along any of the three orientations investigated, a volume nucleation process ($n = 3$) became evident on intermediate time scales of $t > 10^{-4}$ s. The fact that $n = 3$ for this process indicates that nucleation is not confined to the vicinity of domain boundaries. Rather, it is a volume process: One that has a broad distribution of relaxation times. This is strongly suggestive of heterogeneous nucleation, where nucleation events occur preferentially in the vicinity of defects or random fields. This is consistent with prior studies of soft ferroelectrics by Tan *et al.*,[38] who reported the breakdown of micron-sized ferroelectric domains into PNR with increasing E, and a high ac field-induced relaxor state.

It should be noted that these two sequential nucleation events were separated by a hibernation period. With increasing the field to $E \gg E_c$, the two sequential events began (i) merging together, (ii) sharpening their relaxation time distributions, and (iii) shifting the average τ to noticeably shorter times. At higher fields of $E \gg E_c$, switching seemingly occurs by a ballistic mechanism.

C. Summary

The polarization response of variously oriented PZN–x%PT crystals has been investigated over broad time and field ranges. The results unambiguously demonstrate the presence of extremely broad relaxation time distributions for switching, which can extend over a decade(s) in orders of magnitude in time. The polarization response over the time domain of $10^{-8} < t < 10^{2}$ s was well fit to stretched exponential functions. Multiple stretched exponential contributions were required: One under moderate E which was dimension-

ally confined ($n=2$) to domain walls, and a second under higher E which was a volume process ($n=3$) that was geometrically unconfined with nucleation preferentially occurring in the vicinity of defects or random fields.

ACKNOWLEDGMENTS

The authors gratefully acknowledge the support of the Office of Naval Research under Grant Nos. N000140210340, N000140210126, and MURI N000140110761.

[1] S. Park and T. R. Shrout, J. Appl. Phys. **82**, 1804 (1997).
[2] S. Park and T. R. Shrout, IEEE Trans. Ultrason. Ferroelectr. Freq. Control **44**, 1140 (1997).
[3] B. Noheda, J. A. Gonzalo, L. E. Cross, R. Guo, S. E. Park, D. E. Cox, and G. Shirane, Phys. Rev. B **61**, 8687 (2000).
[4] B. Noheda, D. Cox, G. Shirane, J. Gonzalo, and L. E. Cross, Appl. Phys. Lett. **74**, 2059 (1999).
[5] B. Noheda, D. Cox, G. Shirane, E. Park, L. E. Cross, and Z. Zhong, Phys. Rev. Lett. **86**, 3891 (2001).
[6] K. Ohwada, K. Hirota, P. Rehrig, Y. Fujii, and G. Shirane, Phys. Rev. B ; arXiv: cond-mat/0207726.
[7] D. Viehland and J. F. Li, J. Appl. Phys. **92**, 7690 (2002).
[8] H. Fu and R. Cohen, Nature (London) **403**, 281 (2000).
[9] L. Bellaiche, A. Garcia, and D. Vanderbilt, Phys. Rev. Lett. **84**, 5427 (2000).
[10] D. Viehland, J. Appl. Phys. **88**, 4794 (2000).
[11] D. Viehland and J. Powers, J. Appl. Phys. **89**, 1820 (2001).
[12] D. Viehland, J. Powers, and J. F. Li, J. Appl. Phys. **90**, 2479 (2001).
[13] W. J. Merz, Phys. Rev. **95**, 690 (1954).
[14] M. E. Drougard, J. Appl. Phys. **31**, 352 (1960).
[15] R. C. Miller and G. Weinreich, Phys. Rev. **117**, 1460 (1960).
[16] V. Shur, E. Rumyantsev, and S. Makarov, J. Appl. Phys. **84**, 445 (1998).
[17] Y. Ishibashi and Y. Takagi, J. Phys. Soc. Jpn. **31**, 506 (1971).
[18] A. Levstik, M. Kosec, V. Bobnar, C. Filipic, and J. Holc, Jpn. J. Appl. Phys., Part 1 **36, 5A**, 2744 (1997).
[19] Y. Ishibashi, Integr. Ferroelectr. **2**, 41 (1992).
[20] T. Song, S. Aggarwal, Y. Gallais, B. Nagaraj, R. Ramesh, and J. Evans, Appl. Phys. Lett. **73**, 3366 (1998).
[21] I. Boscolo and S. Cialdi, J. Appl. Phys. **91**, 6125 (2002).
[22] D. Viehland and J. F. Li, J. Appl. Phys. **90**, 2995 (2001).
[23] D. Viehland and Y. Chen, J. Appl. Phys. **88**, 6696 (2000).
[24] J. M. Benedetto, R. A. Moore, and F. B. McLean, J. Appl. Phys. **75**, 460 (1994).
[25] J. Dalton, Phys. Rev. **133A**, 1034 (1964).
[26] J. F. Scott, L. Kammerdiner, M. Parris, S. Traynor, V. Ottenbacher, A. Shawabkeh, and W. Oliver, J. Appl. Phys. **64**, 787 (1988).
[27] J. F. Scott, *Ferroelectric Memories* (Springer, Berlin, 2000).
[28] Y. Imry and S. Ma, Phys. Rev. Lett. **35**, 1399 (1975).
[29] T. Nattermann and J. Villain, Phase Transitions **11**, 5 (1988).
[30] J. Villian, J. Phys. (France) **46**, 1843 (1985).
[31] J. Mydosh, *Spin Glasses, An Experimental Introduction* (Taylor and Francis, London, 1993).
[32] S. Hutton, U. Hochli, and M. Magilone, in *Relaxation in Complex Systems and Related Topics*, edited by I. Campbell and C. Biovannella (Plenum, New York, 1990), p. 289.
[33] W. Kleeman, Int. J. Mod. Phys. **7**, 2469 (1993).
[34] G. A. Smolenskii and A. Agranovskaya, Sov. Phys. Solid State **1**, 1429 (1960).
[35] L. E. Cross, Ferroelectrics **151**, 305 (1994).
[36] J. Chen, H. Chan, and M. Harmer, J. Am. Ceram. Soc. **72**, 593 (1989).
[37] D. Viehland, N. Kim, Z. Xu, and D. Payne, J. Am. Ceram. Soc. **78**, 2481 (1995).
[38] Q. Tan and D. Viehland, Phys. Rev. B **53**, 14103 (1996).
[39] The authors acknowledge that the control units and high-voltage test heads were designed and built by Paul Moses, State College, PA 16801.
[40] D. Viehland, M. Wuttig, and L. E. Cross, J. Appl. Phys. **68**, 2916 (1991).
[41] D. Viehland, M. Wuttig, and L. E. Cross, Philos. Mag. B **64**, 335 (1991).
[42] D. Viehland, M. Wuttig, and L. E. Cross, Ferroelectrics **120**, 71 (1991).